

Make instruments to plague us

6. TOOLS FOR MOLECULAR ELECTRONICS

Source
No Spec: Text
W: Wikipedia

Microscopy

Three Different Classes:

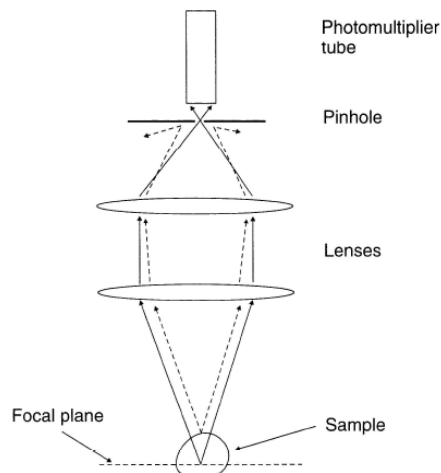
- Optical Microscopy
- Electron Microscopy
- Scanning Probe Microscopy

Two Different Methods:

- Wide-field irradiation (Standard Optical Microscope, TEM)
- Scanning of a fine Beam over the Sample (Confocal Laser Scanning Microscopy, SEM)

Optical Microscopy

- Organic compounds suffers from (1) low image contrast in standard bright field optical microscopy, (2) diffraction limit $d = \lambda/2\theta$ (200 nm), and (3) image blurring by out-of-focus light
- **Dark Field Microscopy**: exclude the directly transmitted light and collects only the scattered light
- **Phase Contrast Microscopy**: Use of phase plate; converts small phase shift generated in the specimen into the intensity contrast
- **Confocal Microscopy**: eliminate out-of-focus light (optical sectioning), recently CLSM (confocal laser scanning microscope: combines fluorescence)
- **Scanning Near-Field Optical Microscopy** (SNOM or NSOM): subwavelength-size aperture, beyond the resolution limit, one of the SPM family
- Fluorescence Microscope, Polarizing Optical Microscope



Confocal

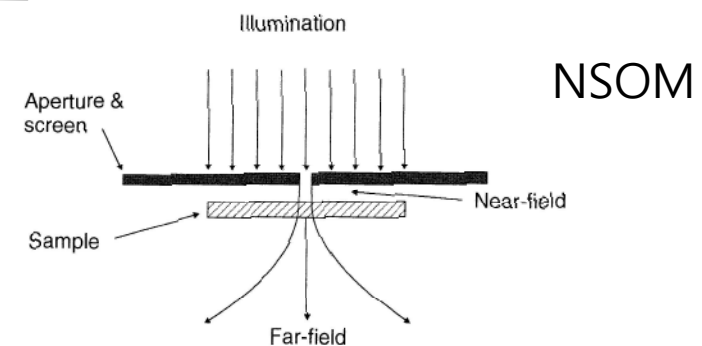
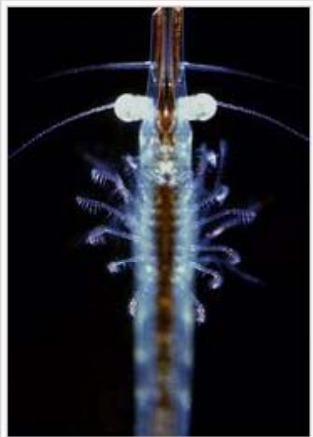


Figure 6.2 Schematic diagram showing the principles of scanning near-field optical microscopy (SNOM or NSOM).

Figure 6.1 A confocal optical microscopy system. The small pinhole permits data collection from a thin optical plane within the sample. Points that are outside the plane of focus will have a different secondary focal plane and therefore most of the light is deflected (dashed lines).

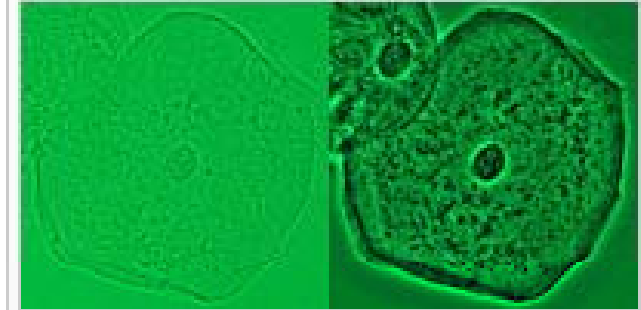
In the near field, resolution is determined by the aperture diameter. Essentially, this is the use of evanescent field



Dark field microscopy produces an image with a dark background.

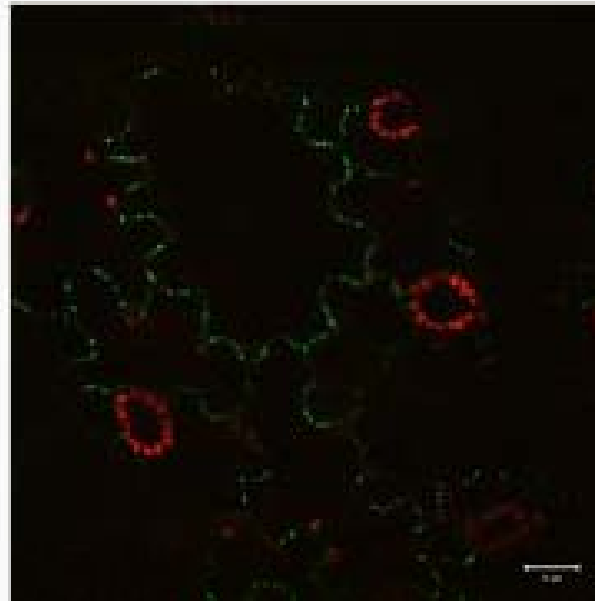
Dark Field Microscopy

W



Epithelial cell in brightfield (BF) using a Plan Fluor 40x lens (NA 0.75) (left) and with phase contrast using a DL Plan Achromat 40x (NA 0.65) (right). A green interference filter is used for both images.

Phase Contrast Microscopy



An example of a GFP fusion protein.

CLSM

Electron Microscopy

- Electron wavelength ($\sim 3.7 \times 10^{-3}$ nm for 100 kV) gives atomic resolution
- Transmission Electron Microscopy (TEM): resolution ~ 0.05 nm
- Scanning Electron Microscopy (SEM)
- Scanning Transmission Electron Microscopy (STEM): reduced radiation damage
- **Sampling of molecular materials:** metal coating for SEM, thin film coating on C-coated Cu grid for TEM

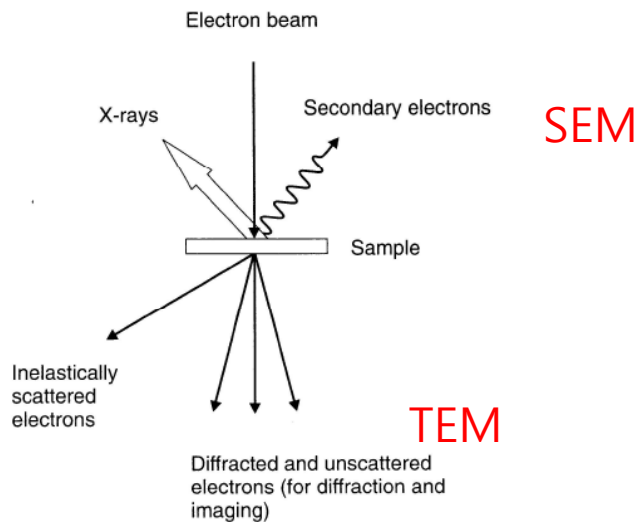


Figure 6.3 Interaction of an electron beam with a sample.

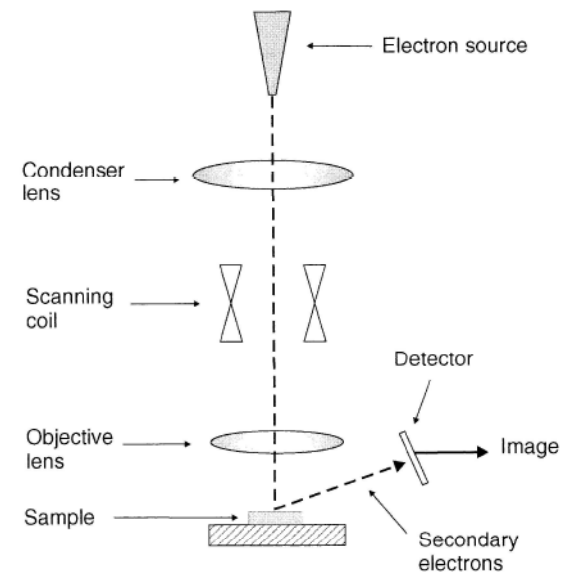


Figure 6.4 Schematic diagram of a scanning electron microscope.

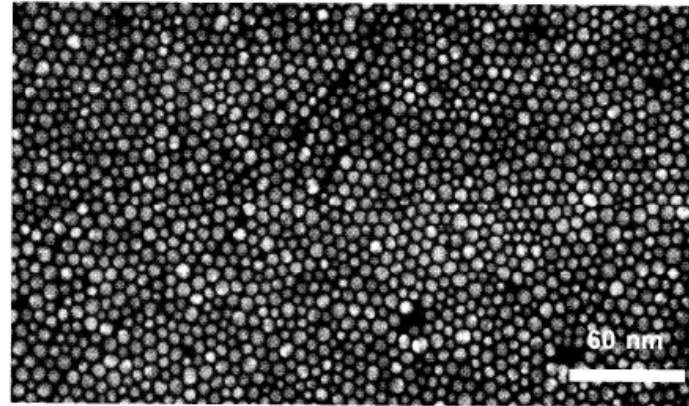
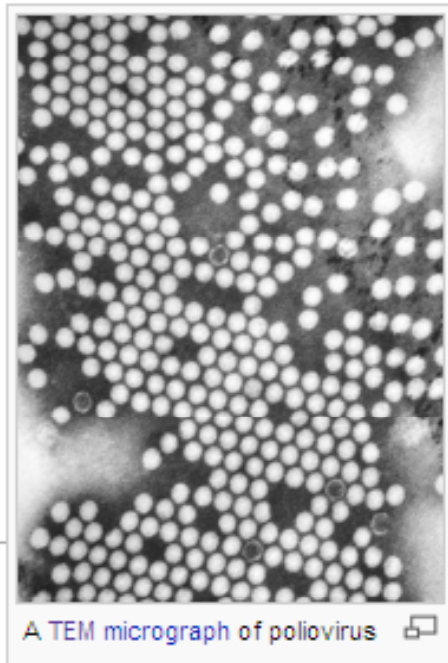


Figure 6.5 Transmission electron micrograph of Au nanoparticles deposited on a carbon-coated microscope grid using the LB technique [1].



Poliomyelitis is caused by infection with a member of the genus Enterovirus known as **poliovirus (PV)**. This group of RNA viruses prefers to inhabit the gastrointestinal tract.[1] PV infects and causes disease in humans alone.[3] Its structure is very simple, composed of a single (+) sense RNA genome enclosed in a protein shell called a capsid.[3] In addition to protecting the virus's genetic material, the capsid proteins enable poliovirus to infect certain types of cells.



W

X-ray Reflection from LB Films

- d_{001} of LB multilayer film of cadmium octadecanoate is ~ 5.0 nm \rightarrow giving $\theta \sim 1^\circ$ for the first order Bragg peak

$$n\lambda = 2d_{001} \sin \theta$$

$n=1$, Y-type LB thus 2x molecular length

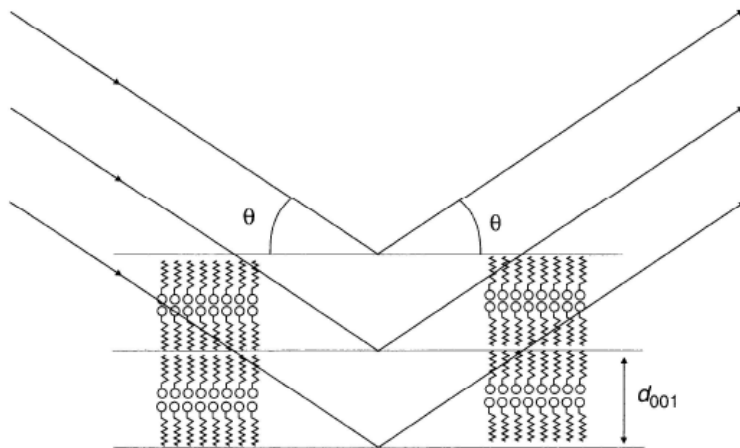


Figure 6.6 Bragg reflection from LB film planes with spacing d_{001} .

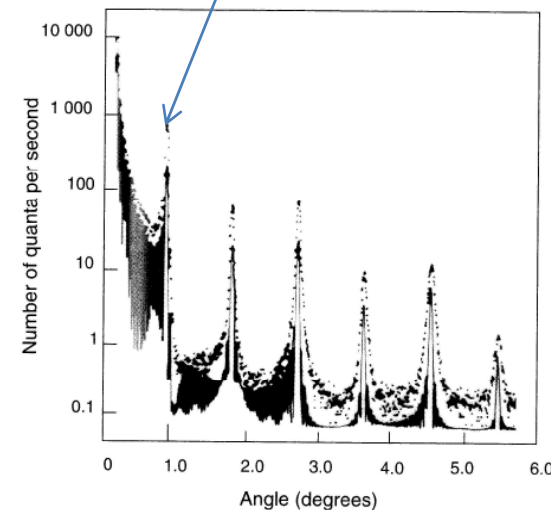


Figure 6.7 X-ray diffraction data from a 43-layer LB film of perdeuterated manganese octadecanoate on a silicon substrate. Experimental values are shown as points. The solid curve is based on calculation and is displaced from the data points [2]. Reprinted with permission from *Phys. Rev. B*, **23**, Nicklow RM, Pomerantz M, Segmüller A, 'Neutron diffraction from small numbers of Langmuir-Blodgett monolayers of manganese stearate', pp. 1081-1087, Copyright (1981), American Physical Society.

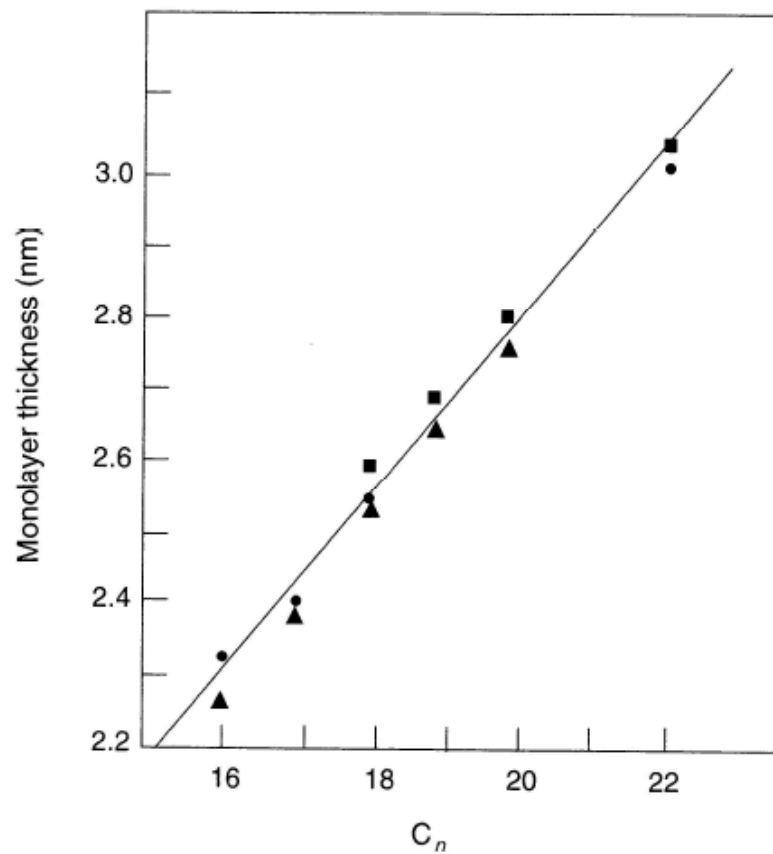
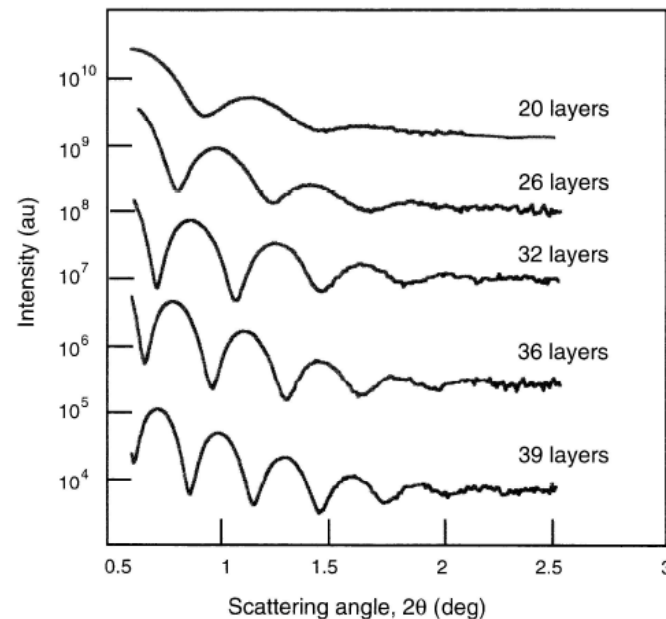


Figure 6.8 Monolayer thickness, obtained from X-ray diffraction experiments, versus number of carbon atoms in the molecule for salts of long-chain fatty acids [3]. Reprinted from Petty MC, *An Introduction to Langmuir-Blodgett Films*, Cambridge: Cambridge University Press, 1996, p. 100.

Kiessig Fringes

- X-ray interference pattern from thin film at a glancing angle (few tenths of a degree) close to the critical angle Θ_c : NOT the Bragg diffraction



$$\sin \theta_m = m \frac{\lambda}{2t}$$

where θ_m is the m-th fringe max.
and t is the film thickness.

Absence of Bragg peaks means
poor degree of L to L ordering.

Figure 6.9 X-ray diffraction data for different numbers of layers of alternating anionic and cationic polyelectrolyte films deposited by the layer-by-layer technique. Kiessig interference fringes are evident. Reprinted from *Protein Architecture*, Lvov Y, p. 133, Copyright (1999), with permission from Taylor & Francis Group LLC.

Electron Diffraction: LB Films

- Structure normal to the film plane: grazing angle e-diffraction
- In-plane structural feature: transmission geometry: orthorhombic R(001) packing of the subshell

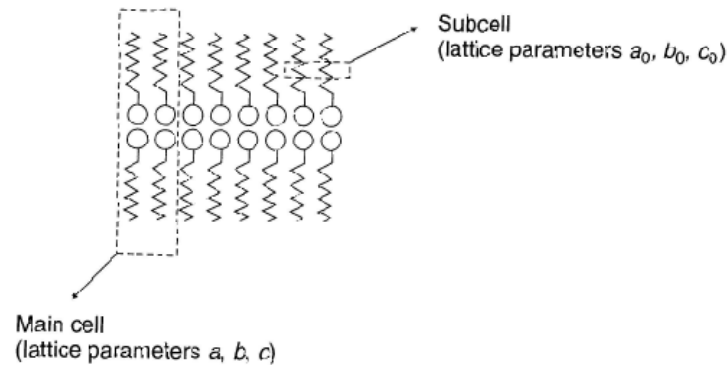
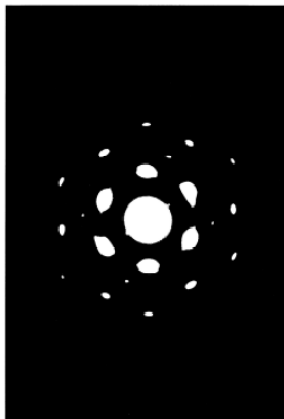


Figure 6.10 Main cell and subcells for fatty acid multilayers.



File history and other information for this document. The following information is provided for your reference only. All rights reserved. All other trademarks and registered trademarks are the property of their respective owners. All other trademarks and registered trademarks are the property of their respective owners.

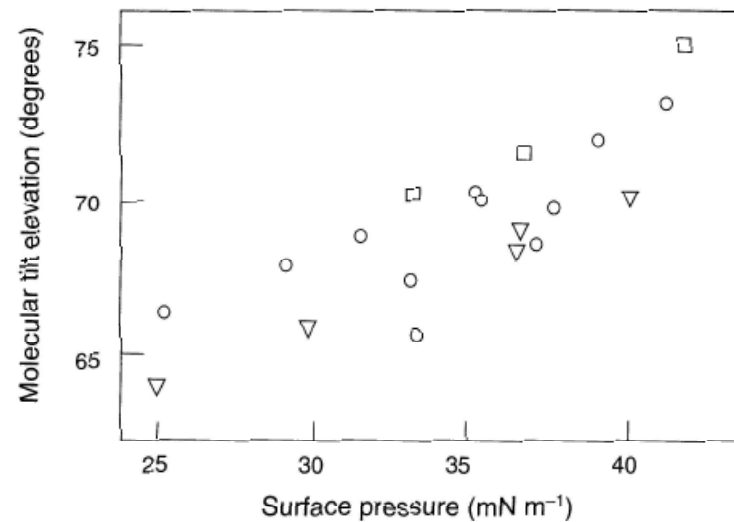


Figure 6.12 Molecular tilt (measured from substrate plane) versus deposition surface pressure for 22-tricosenoic acid LB films. □, deposition pH 7; ○, pH 3. Reprinted from *Thin Solid Films*, **161**, Peterson IR, Russell GJ, Earls JD, Girling IR. 'Surface pressure dependence of molecular tilt in Langmuir-Blodgett films of 22-tricosenoic acid', pp. 325-331, Copyright (1988), with permission from Elsevier. ▽, pH 7. Data from Barnes and Sambles [12].

IR Spectroscopy

- Probes the vibrational features of given functional groups: quantized vibrational levels, specific absorption of IR frequency
- Normal modes: one in which all the nuclei undergo the same frequency motion and move in phase ($3N-5$ for linear molecule and $3N-6$ for nonlinear molecule: thus **3 normal modes for water**)
- Only the component of radiation polarized in the direction of the **transition dipole moment** will induce a change from one vibrational energy level to another .

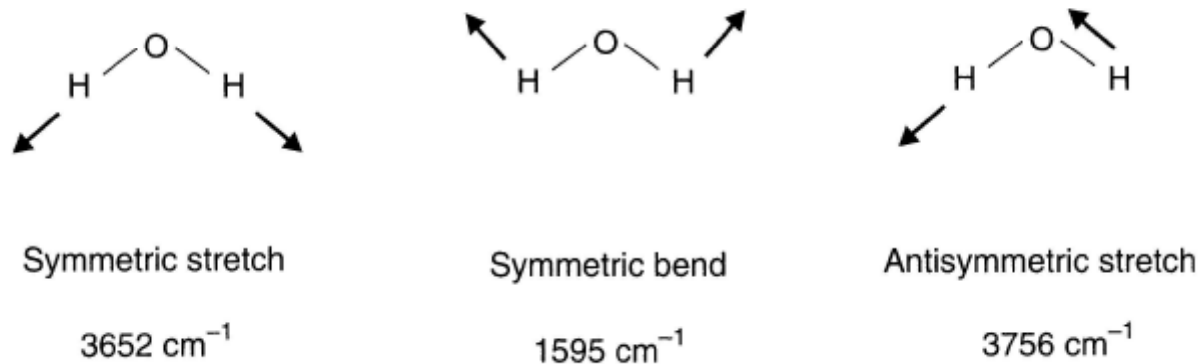
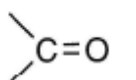
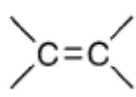


Figure 6.13 Three fundamental vibrations of the water molecule.

Table 6.1 Characteristic stretching and bending frequencies of molecular groups.

Group	Approximate wavenumber (cm^{-1})
-OH	3600
-NH ₂	3400
=CH ₂	3030
-CH ₃	2960 (antisym. stretch) 2870 (sym. stretch) 1460 (antisym. bend) 1375 (sym. bend)
-CH ₂ -	2920 (antisym. stretch) 2850 (sym. stretch) 1470 (bend)
-C≡C-	2220
	1750-1600
	1650

$$\bar{\nu} = \frac{1}{\lambda} \text{cm}^{-1}$$

$\bar{\nu}$ of 4000 cm^{-1} corresponds to λ of $2.5 \mu\text{m}$

- (a) the projection of the transition dipole moment on the layer plane is monitored
- (b) **ATR** : sample coated on the prism, use of evanescent field
- (c) **RAIRS**: grazing incidence (85-88 degree) : s-pol phase shift of π after reflection, p-pol phase shift of $\pi/2$ after reflection. [Surface selection rule](#)

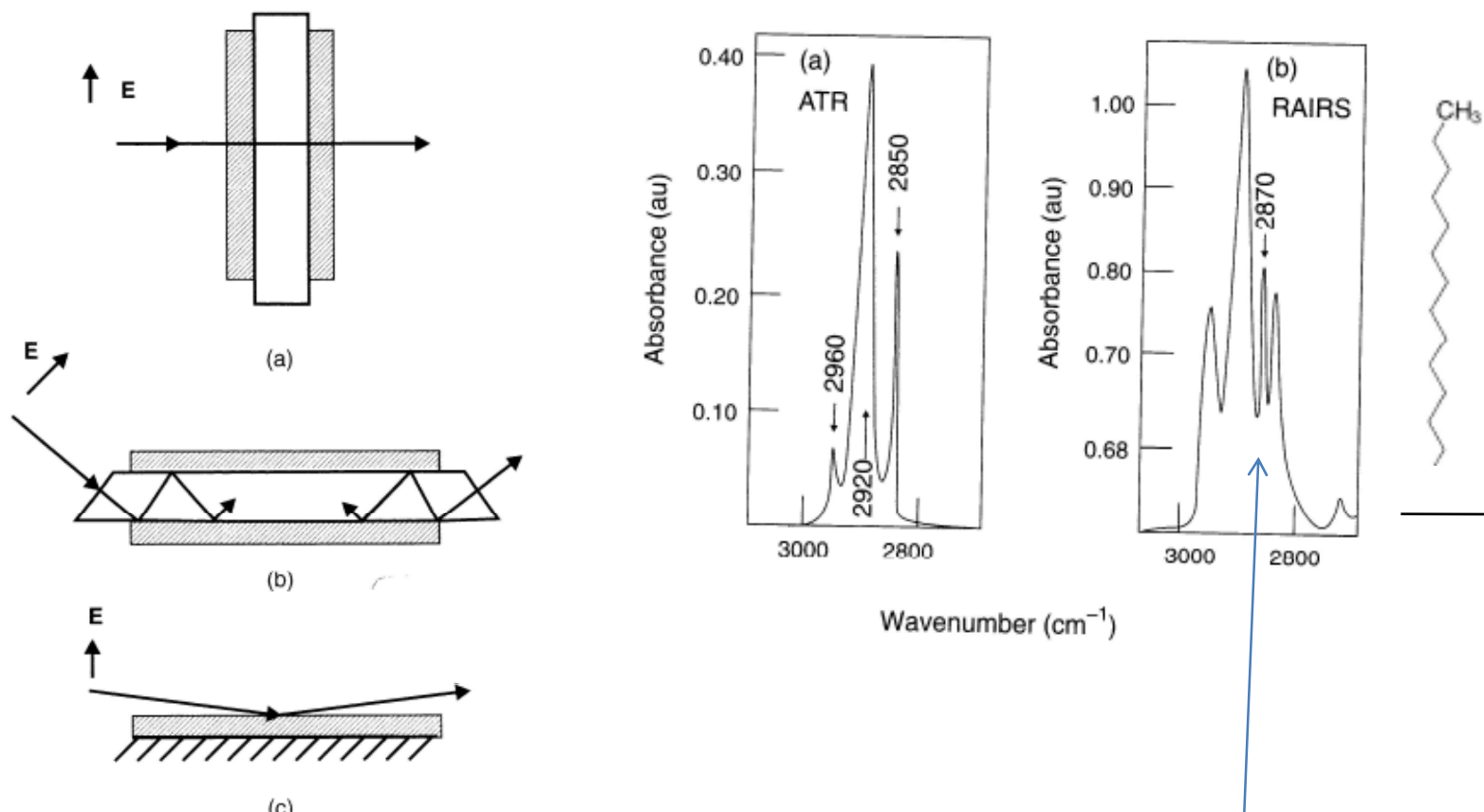


Figure 6.15 Comparison of (a) simple transmission, (b) ATR (attenuated total reflection) and (c) RAIRS (reflection absorption infrared spectroscopy) sampling techniques.

Note that CH₃ stretch at 2870
Gets stronger in RAIRS

Raman Scattering: Inelastic One

- Elastic Scattering (Rayleigh Scattering): $I_s \propto \lambda^4$
- Raman Scattering: inelastic, virtual state, perturbation theory
- Surface –Enhanced Raman Spectroscopy (SERS): interaction with surface plasmon
- To be Raman-active, a molecular rotation or vibration must cause some change in a component of molecular polarizability.

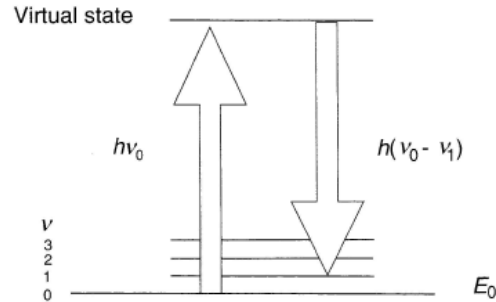
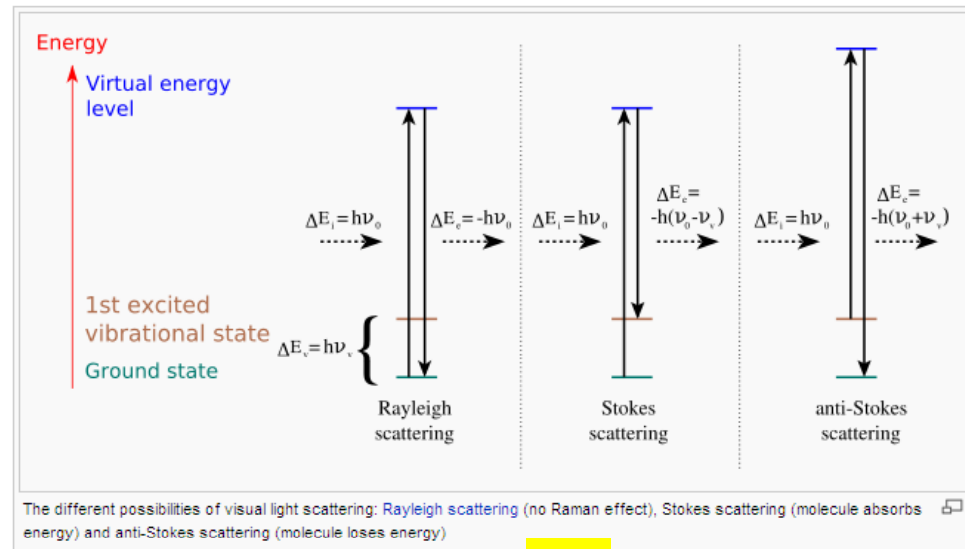


Figure 6.18 Energy level diagram illustrating the Raman scattering process.



Surface Analytical Techniques

Table 6.2 Important surface analytical methods.

Technique	Acronym	Probe beam	Depth probed	Sample beam	Comments
Auger electron spectroscopy	AES	Low-energy (1–10 keV) electrons	0.5–10 nm	Electron energy (20–1000 eV)	Very high surface sensitivity
X-ray photoelectron spectroscopy	XPS	Low-energy X-rays	0.5–5 nm	Photoelectrons	Little surface damage; chemical composition can be determined
Secondary ion mass spectrometry	SIMS	Pulsed ion beam (Ar^+) (few keV)	2 nm–100 μm	Secondary ions	Identification of chemical compounds

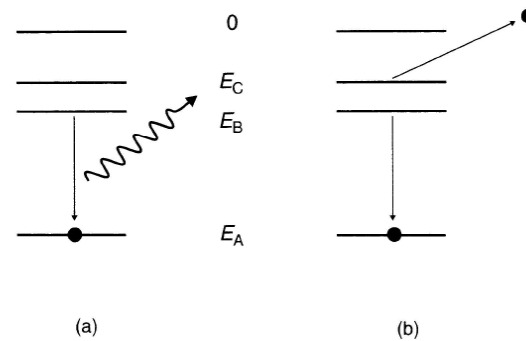


Figure 6.19 Possible processes occurring following the removal of an inner core electron by an incident high energy electron. This vacancy is immediately filled by an electron from a higher energy. (a) X-ray photon emission occurs as the vacancy is filled; (b) Auger effect – the energy is transferred to a second electron, which is subsequently emitted.

Scanning Probe Microscope (SPM)

- Scanning Tunneling Microscope (STM): 1981 Nobel Prize for Physics in 1986, lateral and vertical resolutions of 0.1 and 0.01 nm.
- Atomic Force Microscope (AFM): contact, non-contact, and tapping mode

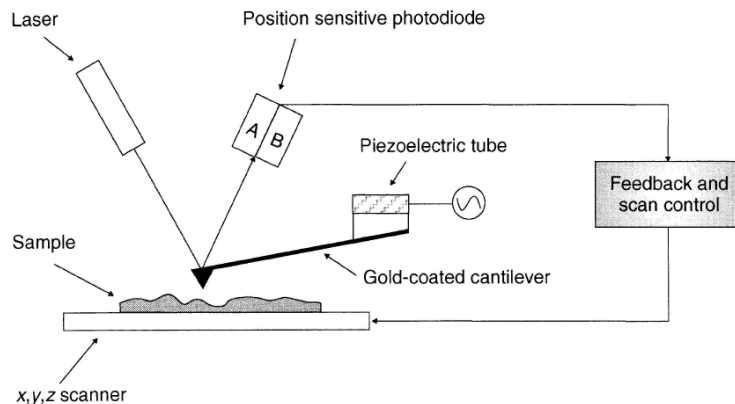
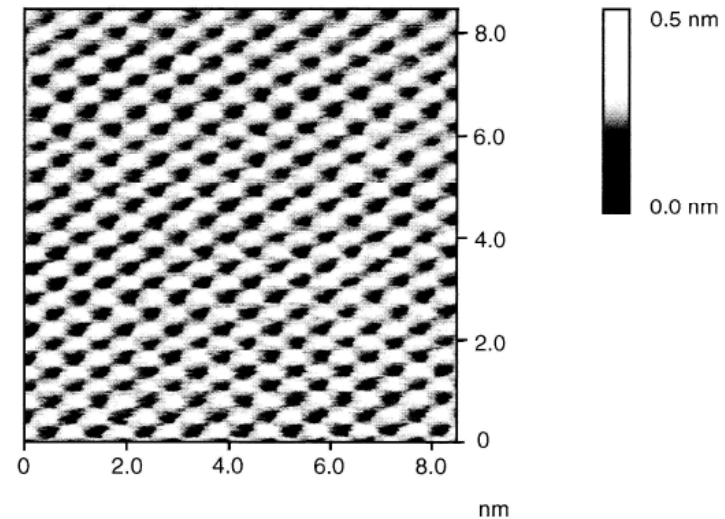
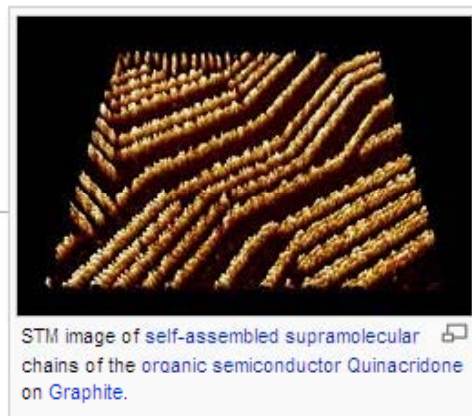


Figure 6.21 Schematic diagram of an atomic force microscope.

Figure 6.22 Atomic force microscope image of a 12-layer 22-tricosenoic acid LB film deposited on silicon. Unfiltered data obtained with a Digital Instruments Nanoscope III. Reprinted with permission from *J. Phys. Chem.* **100**, Evanson SA, Badyal JPS, Pearson C, Petty MC, 'Variation in intermolecular spacing with dipping pressure for arachidic acid LB films', pp. 11672–11674, Copyright (1996) American Chemical Society.

Film Thickness Measurement

Table 6.3 Summary of common methods to determine the thickness of thin organic films.

Technique	Comments
X-ray diffraction	Provides d_{001} lattice spacing. Section 6.3
Ellipsometry	Commercial instruments available; sample refractive index should be known for high accuracy. Chapter 4, Section 4.5.3
Surface plasmon resonance	Sample refractive index should be known. Chapter 4, Section 4.7.2
Capacitance versus number of layers	Provides dielectric thickness. Requires insulating samples. Possibility of damage to organic layer during metallization. Chapter 7, Section 7.3.1
Mechanical probe	Commercial instruments available. Provides metric thickness directly. Organic film may be damaged. Not suitable for monolayer sensitivity